Title

Measurement of the D+→π+π0 and D+→K+π0 branching fractions

Permalink

https://escholarship.org/uc/item/99w3r6sz

Journal

Physical Review D, 74(1)

ISSN

2470-0010

Authors

Aubert, B
Barate, R
Bona, M
et al.

Publication Date

2006-07-01

DOI

10.1103/physrevd.74.011107

Peer reviewed

Measurement of the $D^+ \to \pi^+\pi^0$ and $D^+ \to K^+\pi^0$ branching fractions

B. Aubert,[1] R. Barate,[1] M. Bona,[1] D. Boutigny,[1] F. Couderc,[1] Y. Karyotakis,[1] J. P. Lees,[1] V. Poireau,[1] V. Tisserand,[1]
A. Zghiche,[1] E. Grauges,[2] A. Palano,[3] J. C. Chen,[4] N. D. Qi,[4] G. Rong,[4] P. Wang,[4] Y. S. Zhu,[4] G. Eigen,[5] I. Ofte,[5] B. Stugu,[5]
G. S. Abrams,[6] M. Battaglia,[6] D. N. Brown,[6] J. Button-Shafer,[6] R. N. Cahn,[6] E. Charles,[6] M. S. Gill,[6] Y. Groysman,[6]
R. G. Jacobsen,[6] J. A. Kadyk,[6] L. T. Kerth,[6] Yu. G. Kolomensky,[6] G. Kukartsev,[6] G. Lynch,[6] L. M. Mir,[6] P. J. Oddone,[6]
T. J. Orimoto,[6] M. Pripstein,[6] N. A. Roe,[6] M. T. Ronan,[6] W. A. Wenzel,[6] M. Barrett,[7] K. E. Ford,[7] T. J. Harrison,[7]
A. J. Hart,[7] C. M. Hawkes,[7] S. E. Morgan,[7] A. T. Watson,[7] K. Goetzen,[8] T. Held,[8] H. Koch,[8] B. Lewandowski,[8]
M. Pelizaeus,[8] K. Peters,[8] T. Schroeder,[8] M. Steinke,[8] J. T. Boyd,[9] J. P. Burke,[9] W. N. Cottingham,[9] D. Walker,[9]
T. Cuhadar-Donszelmann,[10] B. G. Fulsom,[10] C. Hearty,[10] N. S. Knecht,[10] T. S. Mattison,[10] J. A. McKenna,[10] A. Khan,[11]
P. Kyberd,[11] M. Saleem,[11] L. Teodorescu,[11] V. E. Blinov,[12] A. D. Bukin,[12] V. P. Druzhinin,[12] V. B. Golubev,[12]
A. P. Onuchin,[12] S. I. Serednyakov,[12] Yu. I. Skovpen,[12] E. P. Solodov,[12] K. Yu Todyshev,[12] D. S. Best,[13] M. Bondioli,[13]
M. Bruinsma,[13] M. Chao,[13] S. Curry,[13] I. Eschrich,[13] D. Kirkby,[13] A. J. Lankford,[13] P. Lund,[13] M. Mandelkern,[13]
R. K. Mommsen,[13] W. Roethel,[13] D. P. Stoker,[13] S. Abachi,[14] C. Buchanan,[14] S. D. Foulkes,[15] J. W. Gary,[15] O. Long,[15]
B. C. Shen,[15] K. Wang,[15] L. Zhang,[15] H. K. Hadavand,[16] E. J. Hill,[16] H. P. Paar,[16] S. Rahatlou,[16] V. Sharma,[16]
J. W. Berryhill,[17] C. Campagnari,[17] A. Cunha,[17] B. Dahmes,[17] T. M. Hong,[17] D. Kovalskyi,[17] J. D. Richman,[17]
T. W. Beck,[18] A. M. Eisner,[18] C. J. Flacco,[18] C. A. Heusch,[18] J. Kroseberg,[18] W. S. Lockman,[18] G. Nesom,[18] T. Schalk,[18]
B. A. Schumm,[18] A. Seiden,[18] P. Spradlin,[18] D. C. Williams,[18] M. G. Wilson,[18] J. Albert,[19] E. Chen,[19] A. Dvoretskii,[19]
D. G. Hitlin,[19] I. Narsky,[19] T. Piatenko,[19] F. C. Porter,[19] A. Ryd,[19] A. Samuel,[19] R. Andreassen,[20] G. Mancinelli,[20]
B. T. Meadows,[20] M. D. Sokoloff,[20] F. Blanc,[21] P. C. Bloom,[21] S. Chen,[21] W. T. Ford,[21] J. F. Hirschauer,[21] A. Kreisel,[21]
U. Nauenberg,[21] A. Olivas,[21] W. O. Ruddick,[21] J. G. Smith,[21] K. A. Ulmer,[21] S. R. Wagner,[21] J. Zhang,[21] A. Chen,[22]
E. A. Eckhart,[22] A. Soffer,[22] W. H. Toki,[22] R. J. Wilson,[22] F. Winklmeier,[22] Q. Zeng,[22] D. D. Altenburg,[23] E. Feltresi,[23]
A. Hauke,[23] H. Jasper,[23] B. Spaan,[23] T. Brandt,[24] V. Klose,[24] H. M. Lacker,[24] W. F. Mader,[24] R. Nogowski,[24] A. Petzold,[24]
J. Schubert,[24] K. R. Schubert,[24] R. Schwierz,[24] J. E. Sundermann,[24] A. Volk,[24] D. Bernard,[25] G. R. Bonneaud,[25]
P. Grenier,[25,*] E. Latour,[25] Ch. Thiebaux,[25] M. Verderi,[25] D. J. Bard,[26] P. J. Clark,[26] W. Gradl,[26] F. Muheim,[26] S. Playfer,[26]
A. I. Robertson,[26] Y. Xie,[26] M. Andreotti,[27] D. Bettoni,[27] C. Bozzi,[27] R. Calabrese,[27] G. Cibinetto,[27] E. Luppi,[27]
M. Negrini,[27] A. Petrella,[27] L. Piemontese,[27] E. Prencipe,[27] F. Anulli,[28] R. Baldini-Ferroli,[28] A. Calcaterra,[28]
R. de Sangro,[28] G. Finocchiaro,[28] S. Pacetti,[28] P. Patteri,[28] I. M. Peruzzi,[28,†] M. Piccolo,[28] M. Rama,[28] A. Zallo,[28]
A. Buzzo,[29] R. Capra,[29] R. Contri,[29] M. Lo Vetere,[29] M. M. Macri,[29] M. R. Monge,[29] S. Passaggio,[29] C. Patrignani,[29]
E. Robutti,[29] A. Santroni,[29] S. Tosi,[29] G. Brandenburg,[30] K. S. Chaisanguanthum,[30] M. Morii,[30] J. Wu,[30] R. S. Dubitzky,[31]
J. Marks,[31] S. Schenk,[31] U. Uwer,[31] W. Bhimji,[32] D. A. Bowerman,[32] P. D. Dauncey,[32] U. Egede,[32] R. L. Flack,[32]
J. R. Gaillard,[32] J. A. Nash,[32] M. B. Nikolich,[32] W. Panduro Vazquez,[32] X. Chai,[33] M. J. Charles,[33] U. Mallik,[33]
N. T. Meyer,[33] V. Ziegler,[33] J. Cochran,[34] H. B. Crawley,[34] L. Dong,[34] V. Eyges,[34] W. T. Meyer,[34] S. Prell,[34]
E. I. Rosenberg,[34] A. E. Rubin,[34] A. V. Gritsan,[35] M. Fritsch,[36] G. Schott,[36] N. Arnaud,[37] M. Davier,[37] G. Grosdidier,[37]
A. Höcker,[37] F. Le Diberder,[37] V. Lepeltier,[37] A. M. Lutz,[37] A. Oyanguren,[37] S. Pruvot,[37] S. Rodier,[37] P. Roudeau,[37]
M. H. Schune,[37] A. Stocchi,[37] W. F. Wang,[37] G. Wormser,[37] C. H. Cheng,[38] D. J. Lange,[38] D. M. Wright,[38] C. A. Chavez,[39]
I. J. Forster,[39] J. R. Fry,[39] E. Gabathuler,[39] R. Gamet,[39] K. A. George,[39] D. E. Hutchcroft,[39] D. J. Payne,[39] K. C. Schofield,[39]
C. Touramanis,[39] A. J. Bevan,[40] F. Di Lodovico,[40] W. Menges,[40] R. Sacco,[40] C. L. Brown,[41] G. Cowan,[41] H. U. Flaecher,[41]
D. A. Hopkins,[41] P. S. Jackson,[41] T. R. McMahon,[41] S. Ricciardi,[41] F. Salvatore,[41] D. N. Brown,[42] C. L. Davis,[42]
J. Allison,[43] N. R. Barlow,[43] R. J. Barlow,[43] Y. M. Chia,[43] C. L. Edgar,[43] M. P. Kelly,[43] G. D. Lafferty,[43] M. T. Naisbit,[43]
J. C. Williams,[43] J. I. Yi,[43] C. Chen,[44] W. D. Hulsbergen,[44] A. Jawahery,[44] C. K. Lae,[44] D. A. Roberts,[44] G. Simi,[44]
G. Blaylock,[45] C. Dallapiccola,[45] S. S. Hertzbach,[45] X. Li,[45] T. B. Moore,[45] S. Saremi,[45] H. Staengle,[45] S. Y. Willocq,[45]
R. Cowan,[46] K. Koeneke,[46] G. Sciolla,[46] S. J. Sekula,[46] M. Spitznagel,[46] F. Taylor,[46] R. K. Yamamoto,[46] H. Kim,[47]
P. M. Patel,[47] S. H. Robertson,[47] A. Lazzaro,[48] V. Lombardo,[48] F. Palombo,[48] J. M. Bauer,[49] L. Cremaldi,[49]
V. Eschenburg,[49] R. Godang,[49] R. Kroeger,[49] J. Reidy,[49] D. A. Sanders,[49] D. J. Summers,[49] H. W. Zhao,[49] S. Brunet,[50]
D. Côté,[50] P. Taras,[50] F. B. Viaud,[50] H. Nicholson,[51] N. Cavallo,[52,‡] G. De Nardo,[52] D. del Re,[52] F. Fabozzi,[52,‡] C. Gatto,[52]
L. Lista,[52] D. Monorchio,[52] P. Paolucci,[52] D. Piccolo,[52] C. Sciacca,[52] M. Baak,[53] H. Bulten,[53] G. Raven,[53] H. L. Snoek,[53]
C. P. Jessop,[54] J. M. LoSecco,[54] T. Allmendinger,[55] G. Benelli,[55] K. K. Gan,[55] K. Honscheid,[55] D. Hufnagel,[55]
P. D. Jackson,[55] H. Kagan,[55] R. Kass,[55] T. Pulliam,[55] A. M. Rahimi,[55] R. Ter-Antonyan,[55] Q. K. Wong,[55] N. L. Blount,[56]
J. Brau,[56] R. Frey,[56] O. Igonkina,[56] M. Lu,[56] C. T. Potter,[56] R. Rahmat,[56] N. B. Sinev,[56] D. Strom,[56] J. Strube,[56]
E. Torrence,[56] F. Galeazzi,[57] A. Gaz,[57] M. Margoni,[57] M. Morandin,[57] A. Pompili,[57] M. Posocco,[57] M. Rotondo,[57]

F. Simonetto,[57] R. Stroili,[57] C. Voci,[57] M. Benayoun,[58] J. Chauveau,[58] P. David,[58] L. Del Buono,[58] Ch. de la Vaissière,[58] O. Hamon,[58] B. L. Hartfiel,[58] M. J. J. John,[58] J. Malclès,[58] J. Ocariz,[58] L. Roos,[58] G. Therin,[58] P. K. Behera,[59] L. Gladney,[59] J. Panetta,[59] M. Biasini,[60] R. Covarelli,[60] M. Pioppi,[60] C. Angelini,[61] G. Batignani,[61] S. Bettarini,[61] F. Bucci,[61] G. Calderini,[61] M. Carpinelli,[61] R. Cenci,[61] F. Forti,[61] M. A. Giorgi,[61] A. Lusiani,[61] G. Marchiori,[61] M. A. Mazur,[61] M. Morganti,[61] N. Neri,[61] G. Rizzo,[61] J. Walsh,[61] M. Haire,[62] D. Judd,[62] D. E. Wagoner,[62] J. Biesiada,[63] N. Danielson,[63] P. Elmer,[63] Y. P. Lau,[63] C. Lu,[63] J. Olsen,[63] A. J. S. Smith,[63] A. V. Telnov,[63] F. Bellini,[64] G. Cavoto,[64] A. D'Orazio,[64] E. Di Marco,[64] R. Faccini,[64] F. Ferrarotto,[64] F. Ferroni,[64] M. Gaspero,[64] L. Li Gioi,[64] M. A. Mazzoni,[64] S. Morganti,[64] G. Piredda,[64] F. Polci,[64] F. Safai Tehrani,[64] C. Voena,[64] M. Ebert,[65] H. Schröder,[65] R. Waldi,[65] T. Adye,[66] N. De Groot,[66] B. Franek,[66] E. O. Olaiya,[66] F. F. Wilson,[66] S. Emery,[67] A. Gaidot,[67] S. F. Ganzhur,[67] G. Hamel de Monchenault,[67] W. Kozanecki,[67] M. Legendre,[67] G. Vasseur,[67] Ch. Yèche,[67] M. Zito,[67] W. Park,[68] M. V. Purohit,[68] J. R. Wilson,[68] M. T. Allen,[69] D. Aston,[69] R. Bartoldus,[69] P. Bechtle,[69] N. Berger,[69] A. M. Boyarski,[69] R. Claus,[69] J. P. Coleman,[69] M. R. Convery,[69] M. Cristinziani,[69] J. C. Dingfelder,[69] D. Dong,[69] J. Dorfan,[69] G. P. Dubois-Felsmann,[69] D. Dujmic,[69] W. Dunwoodie,[69] R. C. Field,[69] T. Glanzman,[69] S. J. Gowdy,[69] M. T. Graham,[69] V. Halyo,[69] C. Hast,[69] T. Hryn'ova,[69] W. R. Innes,[69] M. H. Kelsey,[69] P. Kim,[69] M. L. Kocian,[69] D. W. G. S. Leith,[69] S. Li,[69] J. Libby,[69] S. Luitz,[69] V. Luth,[69] H. L. Lynch,[69] D. B. MacFarlane,[69] H. Marsiske,[69] R. Messner,[69] D. R. Muller,[69] C. P. O'Grady,[69] V. E. Ozcan,[69] M. Perl,[69] A. Perazzo,[69] B. N. Ratcliff,[69] A. Roodman,[69] A. A. Salnikov,[69] R. H. Schindler,[69] J. Schwiening,[69] A. Snyder,[69] J. Stelzer,[69] D. Su,[69] M. K. Sullivan,[69] K. Suzuki,[69] S. K. Swain,[69] J. M. Thompson,[69] J. Va'vra,[69] N. van Bakel,[69] M. Weaver,[69] A. J. R. Weinstein,[69] W. J. Wisniewski,[69] M. Wittgen,[69] D. H. Wright,[69] A. K. Yarritu,[69] K. Yi,[69] C. C. Young,[69] P. R. Burchat,[70] A. J. Edwards,[70] S. A. Majewski,[70] B. A. Petersen,[70] C. Roat,[70] L. Wilden,[70] S. Ahmed,[71] M. S. Alam,[71] R. Bula,[71] J. A. Ernst,[71] V. Jain,[71] B. Pan,[71] M. A. Saeed,[71] F. R. Wappler,[71] S. B. Zain,[71] W. Bugg,[72] M. Krishnamurthy,[72] S. M. Spanier,[72] R. Eckmann,[73] J. L. Ritchie,[73] A. Satpathy,[73] C. J. Schilling,[73] R. F. Schwitters,[73] J. M. Izen,[74] I. Kitayama,[74] X. C. Lou,[74] S. Ye,[74] F. Bianchi,[75] F. Gallo,[75] D. Gamba,[75] M. Bomben,[76] L. Bosisio,[76] C. Cartaro,[76] F. Cossutti,[76] G. Della Ricca,[76] S. Dittongo,[76] S. Grancagnolo,[76] L. Lanceri,[76] L. Vitale,[76] V. Azzolini,[77] F. Martinez-Vidal,[77] Sw. Banerjee,[78] B. Bhuyan,[78] C. M. Brown,[78] D. Fortin,[78] K. Hamano,[78] R. Kowalewski,[78] I. M. Nugent,[78] J. M. Roney,[78] R. J. Sobie,[78] J. J. Back,[79] P. F. Harrison,[79] T. E. Latham,[79] G. B. Mohanty,[79] M. Pappagallo,[79] H. R. Band,[80] X. Chen,[80] B. Cheng,[80] S. Dasu,[80] M. Datta,[80] A. M. Eichenbaum,[80] K. T. Flood,[80] J. J. Hollar,[80] P. E. Kutter,[80] H. Li,[80] R. Liu,[80] B. Mellado,[80] A. Mihalyi,[80] A. K. Mohapatra,[80] Y. Pan,[80] M. Pierini,[80] R. Prepost,[80] P. Tan,[80] S. L. Wu,[80] Z. Yu,[80] and H. Neal[81]

(*BABAR* Collaboration)

[1]*Laboratoire de Physique des Particules, F-74941 Annecy-le-Vieux, France*
[2]*Universitat de Barcelona, Facultat de Fisica Dept. ECM, E-08028 Barcelona, Spain*
[3]*Università di Bari, Dipartimento di Fisica and INFN, I-70126 Bari, Italy*
[4]*Institute of High Energy Physics, Beijing 100039, China*
[5]*University of Bergen, Institute of Physics, N-5007 Bergen, Norway*
[6]*Lawrence Berkeley National Laboratory and University of California, Berkeley, California 94720, USA*
[7]*University of Birmingham, Birmingham, B15 2TT, United Kingdom*
[8]*Ruhr Universität Bochum, Institut für Experimentalphysik 1, D-44780 Bochum, Germany*
[9]*University of Bristol, Bristol BS8 1TL, United Kingdom*
[10]*University of British Columbia, Vancouver, British Columbia, Canada V6T 1Z1*
[11]*Brunel University, Uxbridge, Middlesex UB8 3PH, United Kingdom*
[12]*Budker Institute of Nuclear Physics, Novosibirsk 630090, Russia*
[13]*University of California at Irvine, Irvine, California 92697, USA*
[14]*University of California at Los Angeles, Los Angeles, California 90024, USA*
[15]*University of California at Riverside, Riverside, California 92521, USA*
[16]*University of California at San Diego, La Jolla, California 92093, USA*
[17]*University of California at Santa Barbara, Santa Barbara, California 93106, USA*
[18]*University of California at Santa Cruz, Institute for Particle Physics, Santa Cruz, California 95064, USA*
[19]*California Institute of Technology, Pasadena, California 91125, USA*
[20]*University of Cincinnati, Cincinnati, Ohio 45221, USA*
[21]*University of Colorado, Boulder, Colorado 80309, USA*
[22]*Colorado State University, Fort Collins, Colorado 80523, USA*
[23]*Universität Dortmund, Institut für Physik, D-44221 Dortmund, Germany*
[24]*Technische Universität Dresden, Institut für Kern- und Teilchenphysik, D-01062 Dresden, Germany*

[25]Ecole Polytechnique, LLR, F-91128 Palaiseau, France

[26]University of Edinburgh, Edinburgh EH9 3JZ, United Kingdom

[27]Università di Ferrara, Dipartimento di Fisica and INFN, I-44100 Ferrara, Italy

[28]Laboratori Nazionali di Frascati dell'INFN, I-00044 Frascati, Italy

[29]Università di Genova, Dipartimento di Fisica and INFN, I-16146 Genova, Italy

[30]Harvard University, Cambridge, Massachusetts 02138, USA

[31]Universität Heidelberg, Physikalisches Institut, Philosophenweg 12, D-69120 Heidelberg, Germany

[32]Imperial College London, London, SW7 2AZ, United Kingdom

[33]University of Iowa, Iowa City, Iowa 52242, USA

[34]Iowa State University, Ames, Iowa 50011-3160, USA

[35]Johns Hopkins University, Baltimore, Maryland 21218, USA

[36]Universität Karlsruhe, Institut für Experimentelle Kernphysik, D-76021 Karlsruhe, Germany

[37]Laboratoire de l'Accélérateur Linéaire, IN2P3-CNRS et Université Paris-Sud 11, Centre Scientifique d'Orsay, B.P. 34, F-91898 ORSAY Cedex, France

[38]Lawrence Livermore National Laboratory, Livermore, California 94550, USA

[39]University of Liverpool, Liverpool L69 7ZE, United Kingdom

[40]Queen Mary, University of London, E1 4NS, United Kingdom

[41]University of London, Royal Holloway and Bedford New College, Egham, Surrey TW20 0EX, United Kingdom

[42]University of Louisville, Louisville, Kentucky 40292, USA

[43]University of Manchester, Manchester M13 9PL, United Kingdom

[44]University of Maryland, College Park, Maryland 20742, USA

[45]University of Massachusetts, Amherst, Massachusetts 01003, USA

[46]Massachusetts Institute of Technology, Laboratory for Nuclear Science, Cambridge, Massachusetts 02139, USA

[47]McGill University, Montréal, Québec, Canada H3A 2T8

[48]Università di Milano, Dipartimento di Fisica and INFN, I-20133 Milano, Italy

[49]University of Mississippi, University, Mississippi 38677, USA

[50]Université de Montréal, Physique des Particules, Montréal, Québec, Canada H3C 3J7

[51]Mount Holyoke College, South Hadley, Massachusetts 01075, USA

[52]Università di Napoli Federico II, Dipartimento di Scienze Fisiche and INFN, I-80126, Napoli, Italy

[53]NIKHEF, National Institute for Nuclear Physics and High Energy Physics, NL-1009 DB Amsterdam, The Netherlands

[54]University of Notre Dame, Notre Dame, Indiana 46556, USA

[55]Ohio State University, Columbus, Ohio 43210, USA

[56]University of Oregon, Eugene, Oregon 97403, USA

[57]Università di Padova, Dipartimento di Fisica and INFN, I-35131 Padova, Italy

[58]Universités Paris VI et VII, Laboratoire de Physique Nucléaire et de Hautes Energies, F-75252 Paris, France

[59]University of Pennsylvania, Philadelphia, Pennsylvania 19104, USA

[60]Università di Perugia, Dipartimento di Fisica and INFN, I-06100 Perugia, Italy

[61]Università di Pisa, Dipartimento di Fisica, Scuola Normale Superiore and INFN, I-56127 Pisa, Italy

[62]Prairie View A&M University, Prairie View, Texas 77446, USA

[63]Princeton University, Princeton, New Jersey 08544, USA

[64]Università di Roma La Sapienza, Dipartimento di Fisica and INFN, I-00185 Roma, Italy

[65]Universität Rostock, D-18051 Rostock, Germany

[66]Rutherford Appleton Laboratory, Chilton, Didcot, Oxon, OX11 0QX, United Kingdom

[67]DSM/Dapnia, CEA/Saclay, F-91191 Gif-sur-Yvette, France

[68]University of South Carolina, Columbia, South Carolina 29208, USA

[69]Stanford Linear Accelerator Center, Stanford, California 94309, USA

[70]Stanford University, Stanford, California 94305-4060, USA

[71]State University of New York, Albany, New York 12222, USA

[72]University of Tennessee, Knoxville, Tennessee 37996, USA

[73]University of Texas at Austin, Austin, Texas 78712, USA

[74]University of Texas at Dallas, Richardson, Texas 75083, USA

[75]Università di Torino, Dipartimento di Fisica Sperimentale and INFN, I-10125 Torino, Italy

[76]Università di Trieste, Dipartimento di Fisica and INFN, I-34127 Trieste, Italy

[77]IFIC, Universitat de Valencia-CSIC, E-46071 Valencia, Spain

[78]University of Victoria, Victoria, British Columbia, Canada V8W 3P6

*Also at Laboratoire de Physique Corpusculaire, Clermont-Ferrand, France

†Also with Università di Perugia, Dipartimento di Fisica, Perugia, Italy

‡Also with Università della Basilicata, Potenza, Italy

[79]*Department of Physics, University of Warwick, Coventry CV4 7AL, United Kingdom*
[80]*University of Wisconsin, Madison, Wisconsin 53706, USA*
[81]*Yale University, New Haven, Connecticut 06511, USA*
(Received 16 May 2006; published 21 July 2006)

We present measurements of the branching fractions for the Cabbibo suppressed decays $D^+ \rightarrow \pi^+ \pi^0$ and $D^+ \rightarrow K^+ \pi^0$ based on a data sample corresponding to an integrated luminosity of 124.3 fb^{-1}. The data were taken with the *BABAR* detector at the PEP-II *B* Factory operating on and near the $Y(4S)$ resonance. We find $\mathcal{B}(D^+ \rightarrow \pi^+ \pi^0) = (1.25 \pm 0.10 \pm 0.09 \pm 0.04) \times 10^{-3}$ and $\mathcal{B}(D^+ \rightarrow K^+ \pi^0) = (2.52 \pm 0.47 \pm 0.25 \pm 0.08) \times 10^{-4}$, where the first uncertainty is statistical, the second systematic and the last error is due to the uncertainties in the absolute branching fraction scale for D^+ mesons. This represents the first observation of the doubly Cabibbo-suppressed $D^+ \rightarrow K^+ \pi^0$ decay mode and a new measurement of the $D^+ \rightarrow \pi^+ \pi^0$ branching fraction.

Measurements of rare hadronic D^+ decays provide insight into $SU(3)$ flavor symmetry, QCD dynamics, and weak flavor mixing [1]. Studies of these decays are useful for $D^0 \bar{D}^0$ mixing analyses, which benefit from improved measurements of $D^+ \rightarrow \pi^+ \pi^0$ and $D^+ \rightarrow K^+ K^0$ branching fractions in order to understand the size of the $SU(3)$-violating effects in D meson decays. In addition, doubly Cabibbo-suppressed decays such as $D^0 \rightarrow K^+ \pi^-$ complicate measurements of flavor oscillations in hadronic D^0 decays. Knowledge of the $SU(3)$-related channels reported here can lead to a better understanding of this background. Previous analyses of these D^+ decays were reported by MARK III, CLEO, and FOCUS [2–4].

This analysis is based on data recorded with the *BABAR* detector at the PEP-II asymmetric-energy e^+e^- storage ring at the Stanford Linear Accelerator Center. The data sample corresponds to an integrated luminosity of 124.3 fb^{-1} recorded at center-of-mass (CM) energies $\sqrt{s} = 10.58$ GeV and 10.54 GeV and includes approximately 167×10^6 $e^+e^- \rightarrow c\bar{c}$ events.

The *BABAR* detector is described in detail elsewhere [5]. Charged particle momenta are measured with a 5-layer double-sided silicon vertex tracker (SVT) and a 40-layer drift chamber (DCH), both inside the 1.5 T magnetic field of a superconducting solenoid. A calorimeter (EMC) consisting of 6580 CsI(Tl) crystals measures electromagnetic energy. Charged hadron identification is provided by measurements of the rate of ionization energy loss, dE/dx, in the tracking system and of the Cherenkov angle obtained from a ring-imaging Cherenkov detector (DIRC). The instrumented flux return of the magnet allows discrimination of muons from pions.

We use a Monte Carlo simulation of the *BABAR* detector based on GEANT 4 [6] to validate the analysis and to determine the reconstruction efficiencies for the two signal modes $D^+ \rightarrow \pi^+ \pi^0$ and $D^+ \rightarrow K^+ \pi^0$, as well as for the decay $D^+ \rightarrow K^- \pi^+ \pi^+$,[1] which is used as a reference to

normalize our results. Simulated events are generated with the Pythia event generator [7].

We reconstruct D^+ meson candidates in the signal modes by combining a charged track, identified either as a pion or kaon, with a reconstructed π^0 candidate. Until better knowledge of the overall $e^+e^- \rightarrow D^+X$ production rate is obtained, any measurement of absolute D^+ branching fractions will be limited by the uncertainty in the number of D^+ mesons in the data sample. We avoid this uncertainty by measuring our signal modes relative to the high statistics, well-measured $D^+ \rightarrow K^- \pi^+ \pi^+$ decay mode.

In order to reduce the large amount of combinatorial background in the D^+ signal modes, we include only D^+ mesons that originate from $D^{*+} \rightarrow D^+ \pi^0$ decays. To minimize systematic uncertainties in the reconstruction of the low momentum π^0 from the D^{*+} decay, this is done for both the signal and reference channels.

Only events with at least three charged tracks are selected for this analysis. Charged tracks are required to have a distance of closest approach to the interaction point in the plane transverse to the beam axis of less than 1.5 cm, a distance of closest approach along the beam direction of less than 10 cm, a minimum transverse momentum of 100 MeV/c, and at least 12 DCH hits. All candidate tracks in the reconstructed decay chains must satisfy a set of pion or kaon identification criteria based on the response of the DIRC and the dE/dx measurements in the tracking system.

A pair of energy clusters in the EMC, which are isolated from any charged tracks and have the expected lateral shower shape for photons, is considered a π^0 candidate if both clusters exceed 30 MeV, and the associated invariant mass of the pair is between 0.115 GeV/c^2 and 0.150 GeV/c^2. The energy of the π^0 candidate in the laboratory frame is required to be greater than 0.2 GeV.

We accept a D^+ candidate if its invariant mass falls between 1.7 GeV/c^2 and 2.0 GeV/c^2. In addition we require that the cosine of the helicity angle, θ_h,[2] which is

---

[1]Unless explicitly stated, charge conjugate reactions are implicitly included throughout this paper.

[2]We define θ_h as the angle between the direction of the charged daughter particle of the D^+ decay and the direction of the D^{*+} meson evaluated in the D^+ rest frame.

uniformly distributed for signal events but peaks at ± 1 for background, satisfies $-0.9 < \cos(\theta_h) < 0.8$ for the $D^+ \rightarrow \pi^+ \pi^0$ mode and $-0.9 < \cos(\theta_h) < 0.7$ for the $D^+ \rightarrow K^+ \pi^0$ mode.

Two positively charged pion tracks and a negatively charged kaon track are combined in a vertex fit to form a $D^+ \rightarrow K^- \pi^+ \pi^+$ candidate. We require the chi-squared probability of the vertex fit to be $\mathcal{P} > 0.001$. The candidate is accepted if the invariant mass of the D^+ lies between 1.75 GeV/c^2 and 1.95 GeV/c^2. The smaller range compared with the signal modes reflects the better resolution for this decay mode, which has only charged tracks in the final state.

D^+ candidates are combined with a reconstructed π^0 to select $D^{*+} \rightarrow D^+ \pi^0$ decays. An additional requirement on the center-of-mass momentum, $p_{CM} < 0.45$ GeV/c, is applied to π^0 candidates used in the D^{*+} reconstruction. Only D^{*+} candidates with a mass difference $\Delta m = m_{D^{*+}} - m_{D^+}$ less than 0.155 GeV/c^2 are accepted for this analysis. A requirement on the normalized momentum of the D^{*+} meson,[3] $x_{D^*} > 0.6$, corresponding to a D^* center-of-mass momentum greater than 2.9 GeV/c, eliminates backgrounds from B meson decays and further reduces the combinatorial background. If more than one D^{*+} candidate is reconstructed in an event, we choose the one with the larger x_{D^*} value.

With these requirements applied to Monte Carlo events, we obtain reconstruction efficiencies of 7.8% for the $D^+ \rightarrow \pi^+ \pi^0$ mode, 5.9% for the $D^+ \rightarrow K^+ \pi^0$ mode, and 8.5% for the $D^+ \rightarrow K^- \pi^+ \pi^+$ mode.

We extract the signal yield for each of the three decay modes from the invariant mass distribution of the D^+ candidates with unbinned extended maximum likelihood fits.

For the reference mode, the remaining background in the $K^- \pi^+ \pi^+$ invariant mass distribution is described by a first order polynomial; the signal line shape is modeled by a double Gaussian function. In order to accommodate possible differences in the D^+ momentum distribution in data and Monte Carlo events, a weight function describing the relative change in reconstruction efficiency as a function of the D^+ momentum is included in the likelihood function. Similar corrections are applied to the signal mode fits described below. A second weight function is used in the $D^+ \rightarrow K^- \pi^+ \pi^+$ fit to correct for potential differences between the $K^- \pi^+ \pi^+$ Dalitz plot structure in data and simulated events.

Not all of the D^+ candidates in our sample originate from $D^{*+} \rightarrow D^+ \pi^0$ decays. Some D^+ mesons from other sources can combine with a random π^0 in the event to pass

the Δm requirement. This background is uniformly distributed in Δm; in the invariant mass distribution it peaks at the D^+ mass. While it might be expected that this effect cancels when we calculate branching fraction ratios between signal and reference modes, Monte Carlo studies indicate that this is not the case. A correction, extracted from data, must be applied to compensate for the difference in relative efficiencies between this peaking D^+ background in signal and reference modes, caused mostly by the helicity angle requirement. We use the Δm sideband, shown in Fig. 1, to determine the corrected D^+ yield. The Δm signal region is defined as a 2σ window around the nominal $D^{*+} - D^+$ mass difference; the sideband extends from 5σ above the nominal value to 0.155 GeV/c^2. The signal contains D^+ decays from all sources, while D^+ mesons present in the Δm sideband come from sources other than $D^{*+} \rightarrow D^+ \pi^0$ decays. The invariant mass distributions for the signal and sideband regions are fitted simultaneously with identical signal shapes. The yield in the sideband is constrained to be greater than or equal to zero to avoid an unphysical enhancement of the signal yield should the peaking D^+ background fluctuate low. We scale the D^+ yield from the sideband by the ratio of the integrals under the combinatorial background curve in the signal and sideband regions and subtract this value from the yield in the signal region to extract the net yield of $D^{*+} \rightarrow D^+ \pi^0$, $D^+ \rightarrow K^- \pi^+ \pi^+ (\pi^+ \pi^0, K^+ \pi^0)$ decays corrected for the peaking background.

For the $D^+ \rightarrow \pi^+ \pi^0$ and $D^+ \rightarrow K^+ \pi^0$ signal modes, the double Gaussian signal function is replaced by a bifurcated Gaussian function, which gives a better description of the increased width of the signal toward lower masses,
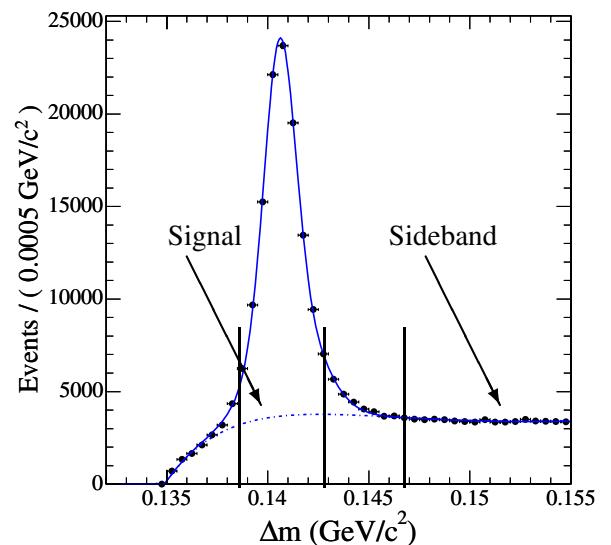
FIG. 1 (color online). Δm distribution for simulated $D^{*+} \rightarrow D^+ \pi^0$, $D^+ \rightarrow K^- \pi^+ \pi^+$ events. The vertical lines mark the signal and sideband regions defined in the text. The solid line shows the result of the fit; the background is given by the dash-dotted line.

---

[3]The normalized momentum x_{D^*} is defined as $x_{D^*} = p_{D^*}^{CM} / \sqrt{s/4 - m_{D^*}^2}$ where $p_{D^*}^{CM}$ is the momentum of the D^* meson in the CM frame and s is the square of the energy of the initial $e^+ e^-$ system.

caused by radiative losses associated with π^0 reconstruction. An exponential function is added to the linear background parametrization to model backgrounds from misreconstructed decays such as $D^+ \rightarrow K_S^0 K^+$ with $K_S^0 \rightarrow \pi^0 \pi^0$ or $D^0 \rightarrow K_S^0 \pi^0$ with $K_S^0 \rightarrow \pi^+ \pi^-$, where two of the three decay products are used to reconstruct a signal mode candidate. This background contribution peaks at low mass, but has a long tail that extends into the D^+ signal region.

The $D^+ \rightarrow K^+ \pi^0$ mode has an additional background. Decays of D_s^+ mesons to $K^+ K_S^0$ final states with the K_S^0 decaying to two neutral pions can cause an excess in the invariant D^+ mass distribution if they are mistakenly reconstructed as $D^+ \rightarrow K^+ \pi^0$, and are combined with a random π^0 to mimic a D^{*+} signal. Based on a Monte Carlo study of $D_s^+ \rightarrow K^+ K_S^0$ events we model this additional background component with a Gaussian function centered at 1.807 GeV/c^2 and with a width of 0.028 GeV/c^2.

Signal and background shapes used in the fits are derived from Monte Carlo events. We minimize systematic uncertainties due to differences between data and the simulation by allowing most parameters to vary in the data fits. The only exceptions are in the $D^+ \rightarrow K^+ \pi^0$ mode where the expected yield is too small to determine the signal shape parameters directly from data. Instead, we use the parameters found in the $D^+ \rightarrow \pi^+ \pi^0$ data fit with the widths reduced by 5%. This correction was obtained in a Monte Carlo study of $D^+ \rightarrow K^+ \pi^0$ and $D^+ \rightarrow \pi^+ \pi^0$ events. The second exception is the shape of the $D_s^+ \rightarrow K^+ K_S^0$ background which is constrained to values obtained from Monte Carlo simulations.

A Monte Carlo sample corresponding to an integrated luminosity of approximately 80 fb^{-1} is used to validate the fit procedure. The branching fraction ratio of $D^+ \rightarrow \pi^+ \pi^0$ to $D^+ \rightarrow K^- \pi^+ \pi^+$ decays in the simulation is 2.8×10^{-2}. With the yields, N_{fit}, extracted from the $D^+ \rightarrow \pi^+ \pi^0$ and $D^+ \rightarrow K^- \pi^+ \pi^+$ fits and the previously determined reconstruction efficiencies ϵ, we obtain

$$\frac{\mathcal{B}(D^+ \rightarrow \pi^+ \pi^0)}{\mathcal{B}(D^+ \rightarrow K^- \pi^+ \pi^+)} = \frac{N_{\text{fit}}(\pi^+ \pi^0) \cdot \epsilon_{K^- \pi^+ \pi^+}}{N_{\text{fit}}(K^- \pi^+ \pi^+) \cdot \epsilon_{\pi^+ \pi^0}} \quad (1)$$

$$= (2.7 \pm 0.1) \times 10^{-2} \quad (2)$$

in good agreement with the expected value. As an example, the $D^+ \rightarrow \pi^+ \pi^0$ fit for simulated data and the different fit components are shown in Fig. 2. We repeat this study for the $D^+ \rightarrow K^+ \pi^0$ mode with the branching fraction ratio in the Monte Carlo sample set to 2.8×10^{-3} and find a value of $(3.1 \pm 0.6) \times 10^{-3}$ for the ratio of the efficiency-corrected yields returned by the $D^+ \rightarrow K^+ \pi^0$ and $D^+ \rightarrow K^- \pi^+ \pi^+$ fits.

Figure 3 shows the fit results for the full data sample. The signal yields are $N_{\text{fit}}(K^- \pi^+ \pi^+) = 101\,380 \pm 415$ for the reference mode, $N_{\text{fit}}(\pi^+ \pi^0) = 1229 \pm 98$ for the
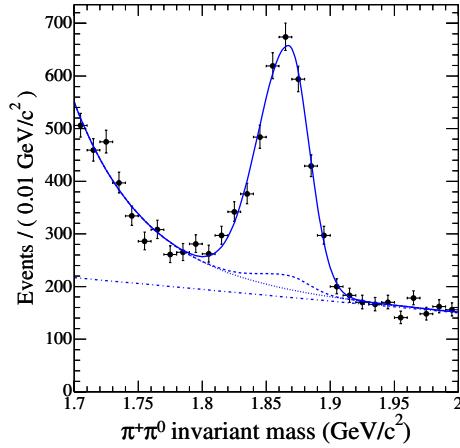

FIG. 2 (color online). $\pi^+ \pi^0$ invariant mass distribution in the $D^+ \rightarrow \pi^+ \pi^0$ signal mode for simulated data. The background is modeled by a first order polynomial (dash-dotted) and an exponential (dotted), while the signal is fitted by a bifurcated Gaussian function. The dashed line shows the peaking D^+ background determined from the Δm sideband fit.

$D^+ \rightarrow \pi^+ \pi^0$ signal mode and $N_{\text{fit}}(K^+ \pi^0) = 189.0 \pm 35.2$ for the $D^+ \rightarrow K^+ \pi^0$ signal mode. The errors are statistical only.

The systematic errors in this analysis include uncertainties in the reconstruction efficiencies as well as the errors associated with the event yields returned by the maximum likelihood fit. Since we measure the branching fraction for $D^+ \rightarrow \pi^+ \pi^0$ and $D^+ \rightarrow K^+ \pi^0$ relative to the $D^+ \rightarrow K^- \pi^+ \pi^+$ reference mode several systematic uncertainties in the efficiencies cancel or are reduced. Individual systematic contributions listed in the following paragraph apply to the measurement of the $\mathcal{B}(D^+ \rightarrow \pi^+ \pi^0)$ to $\mathcal{B}(D^+ \rightarrow K^- \pi^+ \pi^+)$ ratio. Uncertainties of the $\mathcal{B}(D^+ \rightarrow K^+ \pi^0)$ to $\mathcal{B}(D^+ \rightarrow K^- \pi^+ \pi^+)$ ratio are indicated in parentheses if they are different.

The relative systematic error on the efficiencies includes contributions of 1.9% from charged track reconstruction and vertexing, 0.9% (0.4%) from particle identification, 3.2% due to uncertainties in π^0 reconstruction, and 1.1% (1.2%) because of limited Monte Carlo statistics. Uncertainties in reconstruction efficiency of the slow π^0 from D^{*+} decays cancel in the branching fraction ratios. However, because of the π^0 in the final state of the signal modes the D^+ mass resolution differs between signal and reference modes, which has an effect on the shape of the peak in the Δm distribution. Based on a study of simulated events we assign a 5% systematic error due to this effect. The difference between the Δm shapes in data and Monte Carlo events leads to an additional systematic uncertainty of 1.4% for the efficiency ratio. We vary the signal and background parametrizations used in the fits of the D^+ invariant mass distributions and derive a systematic uncertainty of 1.5% for the $D^+ \rightarrow \pi^+ \pi^0$ to $D^+ \rightarrow K^- \pi^+ \pi^+$ efficiency ratio. The fixed signal shape used to
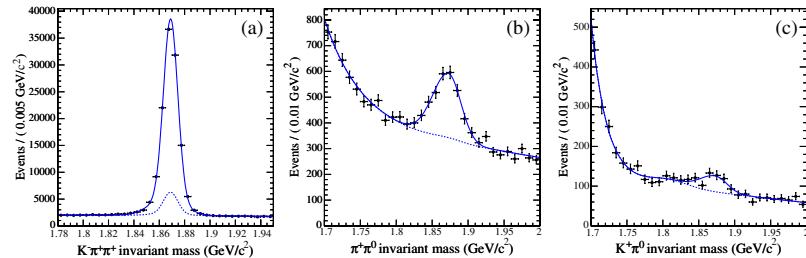
FIG. 3 (color online).   Likelihood fit results for the full data sample for (a) $D^+ \to K^- \pi^+ \pi^+$, (b) $D^+ \to \pi^+ \pi^0$, and (c) $D^+ \to K^+ \pi^0$ decays. The dashed lines show the projected backgrounds in the signal region.

determine the amount of peaking D^+ background in the $D^+ \to K^+ \pi^0$ signal mode causes an additional systematic uncertainty that we estimate by varying the parameters of the Gaussian fit function within their errors and refitting the data. The quadrature sum of both effects gives a 2.7% systematic uncertainty in the $D^+ \to K^+ \pi^0$ to $D^+ \to K^- \pi^+ \pi^+$ efficiency ratio.

We add the individual contributions in quadrature and obtain a total systematic uncertainty for the $D^+ \to \pi^+ \pi^0$ to $D^+ \to K^- \pi^+ \pi^+$ and $D^+ \to K^+ \pi^0$ to $D^+ \to K^- \pi^+ \pi^+$ efficiency ratios of 6.7% and 7.0%, respectively.

The various weights, as well as the signal to sideband scale factor used in the maximum likelihood fits, give rise to systematic uncertainties in the D^+ yield. We study effects caused by the weight functions by varying their parametrizations within their errors, and find that this leads to a systematic error of 0.8% for the two signal modes and 1.2% for the $D^+ \to K^- \pi^+ \pi^+$ reference mode.

The scale factor used for the peaking D^+ background correction, extracted from data using the Δm distribution in the reference mode, is found to be $(34.5 \pm 1.6)\%$. The same scale factor is used for all three D^+ decay modes which results in an additional systematic error of 1.5%. For the $D^+ \to \pi^+ \pi^0$ and $D^+ \to K^- \pi^+ \pi^+$ modes, we combine this in quadrature with the statistical error of the scale factor to obtain a total systematic uncertainty in the amount of peaking D^+ background of 4.9%. In the $D^+ \to K^+ \pi^0$ sample, the D^+ yield in the sideband region fluctuates to a negative value; thus the nominal data fit constrains this component to zero. To estimate the uncertainty due to the peaking D^+ background in this mode we repeat the fit without the constraint and find a difference in signal yield between the constrained and the unconstrained fit of 9.5 events. We use this value as the systematic error on the background-corrected $D^+ \to K^+ \pi^0$ yield.

An additional systematic uncertainty in the $D^+ \to K^+ \pi^0$ analysis is due to the $D_s^+ \to K^+ K_S^0$ background component. Based on the measured branching fraction [8] for this decay we expect 87 ± 58 $D_s^+ \to K^+ K_S^0$ background events in our data sample. This is consistent with the fitted yield of 118 ± 53. When we vary the parameterization of the $D_s^+ \to K^+ K_S^0$ background function in the fit, the reconstructed $D^+ \to K^+ \pi^0$ yield changes by 4.5%, which is taken into account as a systematic error.

With these systematic errors combined in quadrature, the yield in the reference mode is $N_{D^+ \to K^- \pi^+ \pi^+} = 101\,380 \pm 415 \pm 1374$. For the signal modes we find $N_{D^+ \to \pi^+ \pi^0} = 1229 \pm 98 \pm 10$ and $N_{D^+ \to K^+ \pi^0} = 189.0 \pm 35.2 \pm 12.8$.

Following Eq. (2), we combine these measurements with the reconstruction efficiencies to obtain

$$\frac{\mathcal{B}(D^+ \to \pi^+ \pi^0)}{\mathcal{B}(D^+ \to K^- \pi^+ \pi^+)} = (1.33 \pm 0.11 \pm 0.09) \times 10^{-2}$$

and

$$\frac{\mathcal{B}(D^+ \to K^+ \pi^0)}{\mathcal{B}(D^+ \to K^- \pi^+ \pi^+)} = (2.68 \pm 0.50 \pm 0.26) \times 10^{-3}.$$

Using $\mathcal{B}(D^+ \to K^- \pi^+ \pi^+) = 0.094 \pm 0.003$ which is the weighted average of a recent CLEO-c result [9] and the PDG value [8], we derive the branching fractions for the two signal modes

$$\mathcal{B}(D^+ \to \pi^+ \pi^0) = (1.25 \pm 0.10 \pm 0.09 \pm 0.04) \times 10^{-3}$$

and

$$\mathcal{B}(D^+ \to K^+ \pi^0) = (2.52 \pm 0.47 \pm 0.25 \pm 0.08) \times 10^{-4},$$

where the last error is due to the experimental uncertainty in the $D^+ \to K^- \pi^+ \pi^+$ branching fraction. We compute the significance $\mathcal{S}$ of the $D^+ \to K^+ \pi^0$ signal as $\mathcal{S} = \sqrt{2(\ln \mathcal{L}(N_s) - \ln \mathcal{L}(N_s = 0))}$, where $\mathcal{L}(N_s)$ is the maximum likelihood at the nominal fit yield, and $\mathcal{L}(N_s = 0)$ is the value of the likelihood for $N_s = 0$. We include systematic uncertainties by repeating this procedure while varying the fit parameters within their errors. The smallest signal significance obtained in this manner is 6.5 standard deviations.

This represents the first observation of the doubly Cabibbo-suppressed $D^+ \to K^+ \pi^0$ decay mode, and a new measurement of the $D^+ \to \pi^+ \pi^0$ branching fraction.

We can compare our results to theoretical expectations and evaluate the size of $SU(3)$ violation in these decays. In the limit of $SU(3)$, the ratio

$$R_{SU(3)} = 2 \left| \frac{V_{cs}}{V_{cd}} \right|^2 \frac{\Gamma(D^+ \to \pi^+ \pi^0)}{\Gamma(D^+ \to \bar{K}^0 \pi^+)}$$

is expected to approach unity [1]. The extra factor of 2 arises because of the normalization of the π^0 wave function. Combining values for the CKM matrix elements and $\mathcal{B}(D^+ \to \bar{K}^0 \pi^+)$ [10] taken from [8] with our result for $D^+ \to \pi^+ \pi^0$, we find $R_{SU(3)} = 1.54 \pm 0.27$. At the decay amplitude level this corresponds to a 25% deviation from $SU(3)$ symmetry, consistent with theoretical expectations [11].

We can also compare doubly Cabibbo-suppressed decays of charged and neutral D mesons. The two decays $D^+ \to K^+ \pi^0$ and $D^0 \to K^+ \pi^-$ differ only in the flavor of the spectator quark in the D meson. In the absence of D^0 mixing and taking into account that the D^+ decay includes a π^0 in the final state, the ratio of decay rates is expected to be $1/2$. This ratio could be modified by W-annihilation and W-exchange amplitudes that contribute differently to $D^+ \to K^+ \pi^0$ and $D^0 \to K^+ \pi^-$ decays [12]. Experimentally we find

$$\frac{\Gamma(D^+ \to K^+ \pi^0)}{\Gamma(D^0 \to K^+ \pi^-)} = \frac{\mathcal{B}(D^+ \to K^+ \pi^0)}{\mathcal{B}(D^0 \to K^+ \pi^-)} \frac{\tau_{D^0}}{\tau_{D^+}} = 0.71 \pm 0.16$$

where the values for the D lifetimes and $\mathcal{B}(D^0 \to K^+ \pi^-)$ are taken from [8].

[1] L.-L. Chau and H.-Y. Cheng, Phys. Lett. B **333**, 514 (1994).

[2] R. M. Baltrusaitis *et al.*, Phys. Rev. Lett. **55**, 150 (1985).

[3] K. Arms *et al.*, Phys. Rev. D **69**, 071102 (2004); P. Rubin *et al.*, Phys. Rev. Lett. **96**, 081802 (2006).

[4] J. M. Link *et al.*, Phys. Lett. B **618**, 23 (2005).

[5] B. Aubert *et al.*, Nucl. Instrum. Methods Phys. Res., Sect. A **479**, 1 (2002).

[6] S. Agostinelli *et al.*, Nucl. Instrum. Methods Phys. Res., Sect. A **506**, 250 (2003).

[7] T. Sjöstrand *et al.*, Comput. Phys. Commun. **135**, 238 (2001).

[8] S. Eidelman *et al.*, Phys. Lett. B **592**, 1 (2004).

[9] Q. He *et al.*, Phys. Rev. Lett. **95**, 121801 (2005).

[10] This calculation assumes $\mathcal{B}(D^+ \to K_L^0 \pi^+) = \mathcal{B}(D^+ \to K_S^0 \pi^+)$. Bigi and Yamamoto pointed out that due to interference effects these branching fractions could differ by up to 10%. I. Y. Bigi and H. Yamamoto, Phys. Lett. B **349**, 363 (1995).

[11] M. J. Savage, Phys. Lett. B **257**, 414 (1991).

[12] C.-W. Chiang and J. L. Rosner, Phys. Rev. D **65**, 054007 (2002).